Journal of the Serbian Chemical Society
JSCS-info@shd.org.rs • www.shd.org.rs/JSCS
J. Serb. Chem. Soc. *88* (3) 335–348 (2024)
JSCS–5724
Original scientific paper
Published 24 March 2024

Exploring the properties of uranyl nicotinate: Synthesis, characterisation and thermal analysis

MILEICKSON APARECIDO DE ASSIS PIRES, CLAUDIO TEODORO DE CARVALHO and TIAGO ANDRÉ DENCK COLMAN*

Faculty of Exact Sciences and Technology – Federal University of Grande Dourados – UFGD, Dourados, Mato Grosso do Sul, Brazil

(Received 17 August, revised 1 September, accepted 21 September 2023)

Abstract: This study reports the successful synthesis and characterization of a uranyl nicotinate compound, $UO_2(C_6H_4NO_2)_2 \cdot 0.25H_2O$. The compound was synthesized using a metal 1:2 ligand ratio and water as the solvent. The average yield of the compound was 67 %. Thermogravimetric analysis revealed multiple stages of mass loss, including dehydration, nitrogen decomposition and UO_2^{2+} reduction. Fourier-transform infrared spectroscopy confirmed the coordination of the carboxylate group in the compound. Field emission gun scanning electron microscope analysis showed the particles with a regular oval shape. Energy-dispersive X-ray spectroscopy provided semi-quantitative data on the elemental composition of the compound. The major elements identified were uranium, carbon, oxygen and nitrogen. These results contribute to understanding the compound's synthesis, thermal behaviour, molecular composition, particle morphology and elemental composition. Further research can build upon these findings to explore potential applications and develop new compounds with tailored properties.

Keywords: coordination chemistry; actinides; thermoanalytical characterization.

INTRODUCTION

Nicotinic acid derivatives have been extensively studied in coordination chemistry due to their wide spectrum of coordinating modes. These derivatives, such as *N,N*-diethylnicotinamide (DENA), have shown potential as respiratory stimulants. Transition metal complexes with nicotinic acid derivatives and other biochemical-relevant molecules have displayed interesting physical and chemical properties, making them promising candidates for the applications in biological systems.[1]

* Corresponding author. E-mail: tiagocolman@ufgd.edu.br
https://doi.org/10.2298/JSC230817071A

Metal coordination chemistry plays a crucial role in the design and synthesis of novel compounds with desired properties.[2] Crystallography studies have provided valuable insights into the structures of metal complexes. The literature reports studies on the structure of similar compounds Sertçelik *et al.* and Hökelek *et al*.[3–6] Sertçelik *et al.* investigated a manganese complex with monodentate ligands, revealing the intramolecular and the intermolecular hydrogen bonds and π–π interactions.[4] In a related work, a copper complex displayed various hydrogen bonds and C–H···π interactions, adding to our understanding of transition metal complexes.[3] Hökelek *et al.* examined a cobalt complex, emphasizing hydrogen bonds and π–π contacts. They highlighted the significance of nicotinamide in transition metal complexes.[5] Sertçelik and collaborators also describe the structure of the polymeric compound $[Pb(C_{12}H_6N_2O_4)]_n$, the Pb(II) cation is positioned on a mirror plane. It forms *N,N′*-chelation with a 2-2′-bipyridine-5,5′--dicarboxylate (bpdc) anion and coordinates with six oxygen atoms from four carboxyl groups of bpdc anions.[6] Aşkın *et al.* presented a cobalt complex with some intriguing hydrogen bonds and ring motifs, discussing their potential applications in biological systems. The study underscores the relevance of benzoic acid derivatives in coordination chemistry.[7]

Actinide complexation has attracted significant attention due to the unique properties of actinide ions and their potential applications in various fields.[8] The coordination properties of actinide ions, such as uranyl, have been extensively studied.[9] Understanding the coordination environment of actinide complexes is essential for the development of new synthetic methodologies and designing ligands with improved coordination properties.[10]

Synthetic methodologies for the preparation of novel compounds have been the subject of intense research.[11] Microwave-assisted synthesis has emerged as a powerful tool for the rapid and efficient synthesis of various compounds, including metal complexes. This technique offers advantages such as shorter reaction times, higher yields, and improved selectivity.[2] Using the microwave-assisted synthesis, researchers have successfully prepared metal complexes with ligands such as 2-hydroxy-6-methylnicotinic acid.[2]

Ligand design is a critical aspect of coordination chemistry, as ligands play a crucial role in determining the coordination properties of metal complexes. The choice of the right ligand is essential for achieving the desired properties in metal complexes.[12] Distinct types of ligands, such as carbene ligands, imidazole derivatives and phosphine ligands, have been extensively studied for their coordination properties and applications in metal complexes.[12–14]

The coordination properties of metal complexes are influenced by factors such as ligand structure, metal centre, and coordination environment. Understanding the coordination properties of metal complexes is crucial for tailoring their properties for specific applications.[15] Metal–organic frameworks (MOFs)

are an example of coordination polymers that have attracted significant attention due to their unique structures and properties.[16] These frameworks are constructed from metal ions coordinated with organic ligands, and their properties can be fine-tuned by selecting the appropriate structural components.[15]

Research has delved into three-dimensional networks of uranium–carboxylate through covalent and hydrogen bonding. The combination of these bonds is crucial for stability.[17] Organic–inorganic frameworks with uranium and pyridine carboxylate ligands have also been studied, revealing the formation of three-dimensional structures and cation–cation interactions.[18] An organic–inorganic hybrid polymer containing uranyl, nicotinate and molybdate exhibited fluorescent properties. Uranyl, nicotinate and molybdate bonds form the structural basis.[19] Coordination of the uranyl ion with the oxidized calixpyrrole ligand demonstrated the stabilization of the U(VI) oxidation state, with the potential in catalysis and energy storage.[20] The studies by Arnold *et al.* and Kumar *et al.* are related in their investigation of uranyl dication and its reactivity, focused on the reduction and selective oxo group silylation of the uranyl dication. They demonstrated the disruption of the UO_2 bonding by manipulating the uranyl oxo within the molecular cleft, leading to the activation of the exo oxo group towards reductive silylation.[21] They also studied the uranyl dication and its reactivity, specifically in the context of heterobimetallic complexes. They reported the divergent synthesis of heterobimetallic complexes with the uranyl dication and redox-inactive metal cations, which allowed the modulation of the reduction potential of the uranyl ion.[22]

These studies have deepened the understanding of uranium–carboxylate three-dimensional networks and uranium-containing frameworks, highlighting their properties and potential applications. In this article, we will explore the coordination chemistry of nicotinic acid derivatives, the complexation of actinide ions, synthetic methodologies for compounds, ligand design and the coordination properties of metal complexes. In contrast to the existing literature, this study employs a straightforward synthesis route that eliminates the need for extended reaction times or hydrothermal reactors, for instance. Additionally, it extensively investigates the compound's characterisation, particularly focusing on thermoanalytical and microscopic methods. The understanding of these topics is crucial for the development of new synthetic methodologies and the design of novel compounds with tailored properties.

EXPERIMENTAL

Materials

The reagents used for the synthesis of coordination compounds were nicotinic acid (Sigma–Aldrich, purity >99 %), sodium hydroxide (Sigma–Aldrich, purity >99%), and ultrapure water.

Synthesis

The uranyl compound with nicotinic acid (HL) was synthesised with adjustments to the existing methodology in the literature.[23-28] The reaction is a solution of the ligands (diprotonated species derived from the acid) with the solutions prepared from uranyl nitrate.

The acid (2.5 mmol) was dissolved in 30 mL of ultrapure water and slowly neutralised with the drops of NaOH to achieve stoichiometric proportions, as reported in the literature, thereby generating the ligands. The metal solution was prepared by dissolving 1.25 mmol of the metal in 20 mL ultrapure water, maintaining a 1:2 ratio (metal:ligand). The pH of the solutions was adjusted to approximately 5 using a 0.010 mol L^{-1} NaOH solution.

The metal and ligand solutions were heated to 90 °C and slowly mixed dropwise. After the complete mixing, the solution was kept under agitation (100 rpm) and heating (90 °C) for 60 min. Subsequently, the solution was allowed to rest in an open container for evaporation and compound formation. Upon drying, the formed compound was washed with 100 mL of ultrapure water to remove impurities, byproducts, and/or unreacted excess reagents.

Thermal analysis – Simultaneous thermogravimetry and differential scanning calorimetry (TG-DSC)

The TG-DSC curves were obtained using a NETZSCH thermogravimetric analyser, STA 449 F3. It consists of a vertical mass comparator with a capacity of 70.00 µL, a silicon carbide furnace capable of operating in the temperature range of 30 to 1600 °C, and a thermocouple system controlled by Proteus® software. The thermocouples for the sample and reference are made of Pt/Pt–Rh 13 mass %, and the balance sensitivity is 0.2 µg. The system was calibrated according to the manufacturer's specifications. Masses close to 5 mg were used to analyse the samples, and an α-alumina (α-Al_2O_3) sample holder was employed. The purge gas flow (air) was set at 50 mL min^{-1}, with a heating rate of 10 °C min^{-1} and a temperature range of 30–1000 °C.[28-31]

Mid-infrared absorption spectroscopy with Fourier transform (FT-IR)

The infrared spectra were obtained using a Fourier transform infrared spectrophotometer (FT-IR), Nicolet iS10 FT-IR model. The instrument has a resolution of 4 cm^{-1} and can scan the region between 4000–600 cm^{-1} using an attenuated total reflectance (ATR) accessory with a germanium (Ge) crystal.[23,25-29,32]

High-resolution field emission scanning electron microscopy (FEG-SEM) with energy-dispersive X-ray spectroscopy (EDS)

The perimeter and surface area of the formed particles were observed by a MIRA 3 field emission scanning electron microscope (FEG-SEM, Tescan, Czech Republic) with an electron beam current of 15 kV at the field emission gun, generated by a tungsten filament lamp. The particles were previously arranged on a carbon tape and metalised with a 20 mA gold plasma for 150 s to enhance electron passage.[33,34] The analysis of the obtained results was performed with the assistance of ImageJ software.[35]

RESULTS AND DISCUSSION

Synthesis

To observe the distinct characteristics and the formations of compounds derived from metals with similar properties and ligands, the same synthesis pattern was used for all repetitions, with proportions (metal 1:2 ligand) and the use of water as the solvent and reaction medium. The solubility of the metal and the

residues generated at the end of the experiment were observed as relevant in this context.

The synthesis of uranyl coordination compounds was conducted using the corresponding nitrate. The precipitate was washed with distilled water and separated by decantation until the complete elimination of nitrate ions (qualitative test with diphenylamine/H_2SO_4 solution for nitrates).

The pH was maintained at 5 using NaOH throughout the synthesis process, and the temperature was kept around 80 °C for better precipitation. Yang and coworkers reported in their studies that the equilibrium constant for this complex is favourable in solutions with low pH and low L:M ratio (1:1 UO_2L^+), while for the proportions of 1:2 (UO_2L_2), there is a greater affinity for the solutions with higher pH and higher L:M ratio.[36] At the end of ligand addition, the addition of NaOH was also completed, and the pH of the solution with the precipitate stabilised between 2.5 and 3 for all repetitions, according to the observed chemical reaction scheme:

$$2NaC_6H_4NO_2 \xrightarrow[\text{pH 5/80 °C}]{H_2O} \underbrace{UO_2(C_6H_4NO_2)_2 \cdot 0.25H_2O}_{67\ \%} + 2Na^+ + 2NO_3^-$$

The syntheses of coordination compounds with nicotinate and UO_2^{2+} were successfully conducted, producing a significant precipitate for the planned analyses. The characteristic yellow coloration of uranyl compounds was observed (Fig. 1), with an average yield of 67 %.

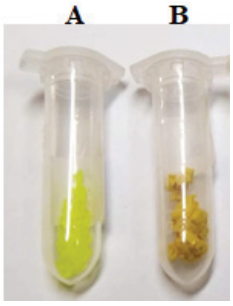

Fig. 1. Comparison of coloration between hexahydrated uranyl nitrate (A) and synthesized uranium nicotinate compound (B).

Thermal characterization: Calculation of molecular formula and theoretical mass loss

Fig. 2 presents the TG-DSC curves of the synthesised compound. A first mass loss is observed between 30–200 °C, accompanied by the endothermic peaks, which are attributed to the dehydration of the compound. This mass loss corresponds to a loss of $0.25H_2O$, which is adsorbed in the complex. The mass loss observed from the beginning of the TG analysis indicates that the water present in the compound is weakly bound.

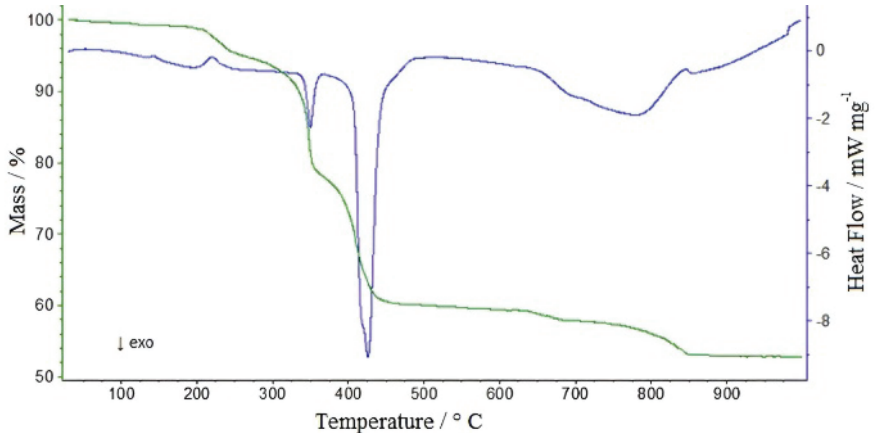

Fig. 2. TG-DSC Curves of $UO_2(C_6H_4NO_2)_2 \cdot 0.25H_2O$, mass 5.2548 mg.

The following calculations were performed to determine the molecular formula and the amount of water present in the compound, about the corresponding theoretical values: UO_2= 270.03 g mol^{-1}; $C_6H_4NO_2$ = 122.11 g mol^{-1}; initial mass = 5.2548 mg; anhydrous mass = 5.1896 mg; experimental residue (TG) = 52.83 %:

$$UO_2(C_6H_4NO_2)_2 \cdot nH_2O \rightarrow UO_2(C_6H_4NO_2)_2 + nH_2O\uparrow:$$

$$514.23:18.02n = 5.1896:0.0652$$

$$n \cong 0.25$$

These calculations were based on the initial and final masses of the compound, allowing the determination of the proportion of each element and the amount of water present. The experimental residue obtained in the TG analysis was 52.83 %. These pieces of information provide a more precise understanding of the composition and the thermochemical characteristics of the synthesised compound, contributing to its characterisation and the understanding of thermal properties. It is important to emphasize that these calculations are complementary to the experimental analyses and help confirm the molecular formula and the presence of water in the compound.

In the second stage of mass loss, the decomposition of nitrogen present in nicotinate is suggested. Based on similar compounds reported in the literature,[26–28] the release of NH_3 is possible to happen at this stage. The stoichiometric calculations support this hypothesis, as the calculated 6.52 % loss closely matches the experimental loss of 5.89 %. These calculations are based on the anhydrous mass obtained in the first stage of the experiment.

Mass: $UO_2(UO_2(C_6H_4NO_2)_2$ = 507,85 g mol^{-1}; NH_3 = 17 g mol^{-1}

$$514.23:2.17 = 5.1896:X$$

$$X = 0{,}3431 \text{ mg}$$

$$\Delta m = 100 \times 0.3475/5.2548 = 6.52\ \%$$

From the third stage to the fifth stage of mass loss, the oxidation of the remaining organic matter and the release of gaseous products during the thermal decomposition are observed.[26,27] Between the fourth and fifth stages of compound decomposition, the formation of a carbonized residue and a carbonate derivative takes place. The compounds were heated until reaching the temperature of the formation of this intermediate, as indicated by the corresponding TG--DSC curves. The test performed with a diluted hydrochloric acid solution, followed by heating of the solution, revealed the presence of the carbonized residue (black solid) and the carbonate derivative, observed through the release of bubbles attributed to the formation of CO_2. This composition stage is considered slow and corresponds to the fifth stage. The last mass loss occurs around 920 °C, and this stage can be attributed to the reduction of UO_2^{2+}, from the oxidation state of 6+ to the formation of UO_2, with an oxidation state of 4+, as the final residue (calculated as 52.06 %, experimentally observed as 52.83 %).

$$UO_2(C_6H_4NO_2)_2 \cdot 0.25H_2O \rightarrow UO_2 + 0.25\ H_2O\uparrow + 2C_6H_4NO_2\uparrow$$

$$518.74:270.03 = 100:X$$

$$X = 52.06\ \%$$

The slightly exothermic enthalpy after the dehydration of uranium nicotinate can be explained by the possible chelation involving the amino nitrogen. This is because the amino nitrogen is less hydrated compared to the carboxylate group, requiring less energy for nitrogen dehydration.[28]

The anhydrous compound remained stable up to 200 °C. The thermal decomposition of the anhydrous compound occurred in five consecutive stages, from the second to the fourth stage, observed at all heating rates, with peaks respectively at 210–220 °C, 340–350 °C and 420–430 °C. For the fifth and sixth stages, higher heating rates are more suitable for observing the mass loss.

Infrared spectroscopy

Fig. 3 presents the Fourier-transform infrared (FT-IR) spectrum in the mid--infrared region of the synthesized complex.

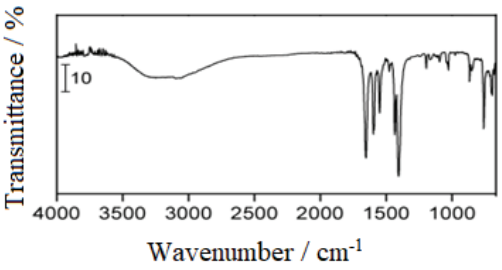

Fig. 3. FT-IR Spectrum of: $UO_2(C_6H_4NO_2)_2 \cdot 0.25H_2O$.

The carboxylate displays two bands: an intense band corresponding to the asymmetric stretching (nas) is observed between 1650 and 1550 cm^{-1}, and a weaker band related to the symmetric stretching (n_s) is observed around 1400 cm^{-1}.[37]

In the case of sodium nicotinate, $Na(C_6H_4NO_2)$, the medium-intensity band at 1566 cm^{-1} and the strong band at 1402 cm^{-1} are attributed to the asymmetric and symmetric frequencies of the carboxylate group, as described in the literature.[27,28]

The analysis of the frequencies of the bands $n_{as}(COO^-)$ at 1543 cm^{-1} and $n_s(COO^-)$ at 1428 cm^{-1} present in the spectrum of the synthesised compound suggests that coordination occurs through the carboxylate group.[27,28,38,39] The calculated values of Δn ($n_{as}(COO^-) - n_s(COO^-)$) for the synthesized compounds are lower than those of the sodium salt (sodium salt Δn = 166 cm^{-1}, the synthesized compound Δn = 115 cm^{-1}), indicating that the coordination of the carboxylate group occurs through a bridging and/or chelating structure. The characteristic bands of the U=O stretch are observed at 930 and 1018 cm^{-1} in the synthesized coordination compound with the significant suppression in its intensity and displacement to lower wavelengths, when compared with uranyl nitrate hexahydrate, which presents these bands at 940 and 1025 cm^{-1} corroborating previous observations in the literature.[40]

Field emission gun scanning electron microscope (FEG-SEM)

Fig. 4 depicts the micrograph of the synthesized compound, captured using a field emission gun scanning electron microscope (FEG-SEM), with a magnification of 55,000 times.

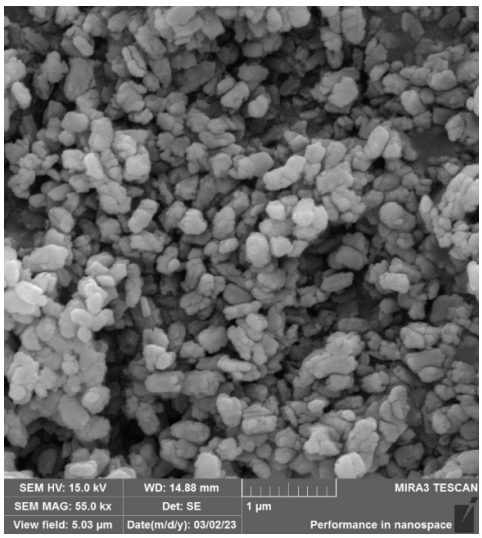

Fig 4. Field emission gun scanning microscopy image of $UO_2(C_6H_4NO_2)_2 \cdot 0.25H_2O$ samples at a magnification of 55,000×.

The analysis of the micrograph reveals that the particles formed exhibit a remarkable regularity in their size and possess an oval shape.

To quantitatively characterize the particles, the histograms illustrating the distribution of the particle perimeter and surface area observed in Fig. 5. The analysis of the data reveals an average particle perimeter of 830 nm and an average surface area of 42.243 nm^2. The obtained data conform to the Gaussian distribution, which provides a statistical description of the particle size distribution based on the perimeter and surface area measurements.

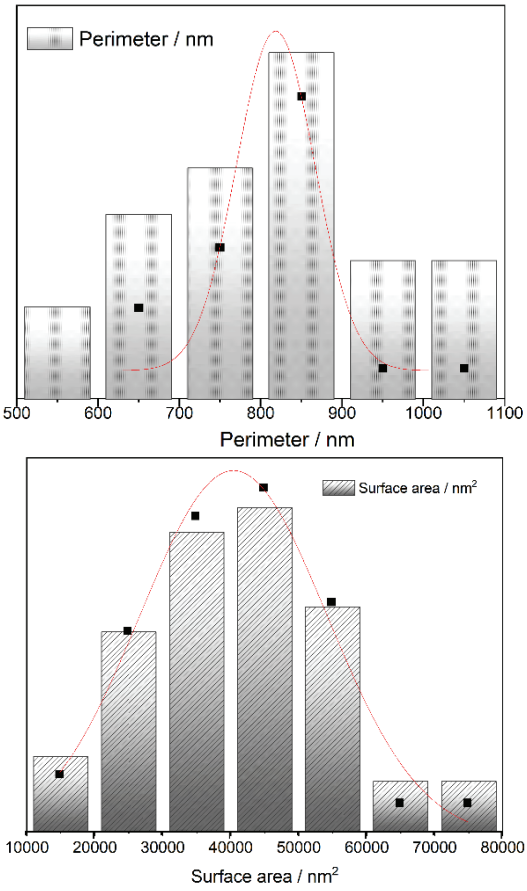

Fig. 5. Histograms and Gaussian distribution curves for the surface area and perimeter of the synthesized particles.

The Gaussian distribution equation for the particle perimeter and surface area can be described as follows:

$$f(x) = \frac{1}{\sigma\sqrt{2\pi}} \exp\left(-\frac{1}{2}\left(\frac{x-y}{\sigma}\right)^2\right) \quad (1)$$

The data obtained from the analysis of the images of the synthesised compound in the ImageJ software were subjected to the following equation: $y = y_0 + (A/(w\times\text{sqrt}(p/2)))\times\exp(-2((x-xc)/w)^2)$. This equation was used to determine the density through the Gaussian distribution of the synthesised particles. The data used to determine the Gaussian distribution are shown in Table I.

TABLE I. Data for Gaussian distribution of the particle perimeter and surface area

Parameter	Surface area	Perimeter
y_0	0.7872±1.50616	5.9202±1.1932
xc	40592.76361±1091.42289	818.37458±36.67738
w	27480.11962±4492.42048	96.53167±98.2148
A	440661.65893±108329.07045	1358.94276±428.49344
Reduced chi-sqare	1.24207	3.97615
R-square (*COD*)	0.97177	0.8965
Adj. *R*-square	0.94354	0.74125

These Gaussian distribution equations provide a mathematical representation of the particle size characteristics observed in the synthesised compound, facilitating a comprehensive understanding of the distribution and the variability of particle sizes within the sample.

The results obtained through EDS analysis reveal a uniform distribution of detected elements in the sample in significant quantities, as evidenced by the elemental distribution map presented in Fig. 6.

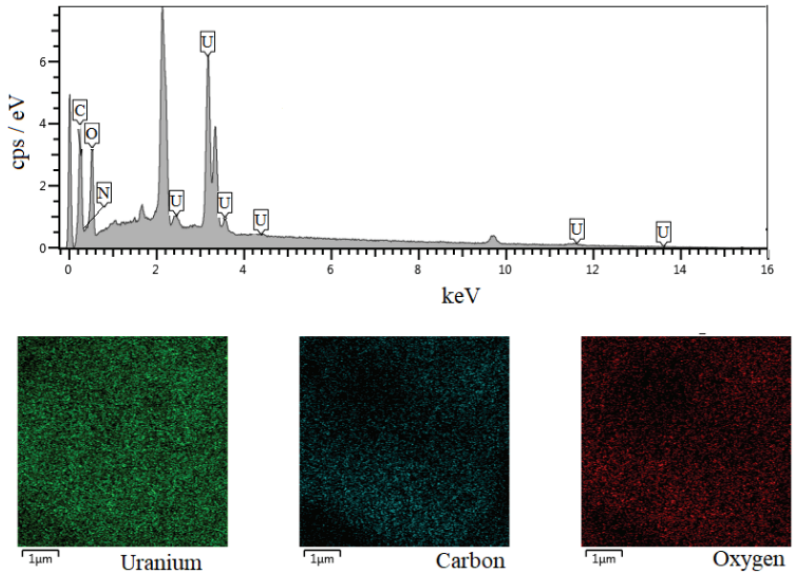

Fig. 6. Dispersive X-ray spectrum and elemental mapping of $UO_2(C_6H_4NO_2)_2\cdot 0.25H_2O$ sample.

The EDS technique enabled the semi-quantitative determination of the composition of the synthesised compound. Uranium was identified as the most predominant element, representing 46.12 % of the mass, followed by carbon at 27.02 %, oxygen at 21.77 %, and nitrogen at 5.09 %. It is important to note that small variations in the percentage values are acceptable, as EDS is unable to quantify hydrogen, which, according to theoretical calculations performed for the synthesised compound, accounts for approximately 2 % of the sample. These results confirm the presence of the expected elements and provide a solid foundation for the understanding of the chemical composition of the synthesised compound.

CONCLUSION

In conclusion, this study successfully synthesised and characterised a uranyl nicotinate compound, $UO_2(C_6H_4NO_2)_2 \cdot 0.25H_2O$. The synthesis process followed a consistent pattern using a metal 1:2 ligand ratio with water as the solvent and reaction medium. The yield of the compound averaged 67 %, indicating the efficient synthesis.

Fourier-transform infrared (FT-IR) spectroscopy confirmed the presence of characteristic bands corresponding to the asymmetric and symmetric stretching frequencies of the carboxylate group. The calculated values of Δn ($n_{as}(COO^-)$ – – $n_s(COO^-)$) indicated a lower value compared to the sodium salt reference, suggesting a bridging and/or chelating coordination structure for the carboxylate group in the synthesised compound.

The field emission gun scanning electron microscope (FEG-SEM) analysis revealed the morphology of the synthesised particles, displaying a regular oval shape. The quantitative analysis of the particle size distribution showed an average particle perimeter of 830 nm and an average surface area of 42,243 nm^2, indicating a relatively uniform particle size within the sample.

The energy-dispersive X-ray spectroscopy (EDS) analysis provided semi--quantitative data on the elemental composition of the synthesised compound. Uranium was identified as the most predominant element, followed by carbon, oxygen, and nitrogen. Although hydrogen could not be quantified by EDS, the theoretical calculations estimated its presence at approximately 2 % in the compound.

These findings contribute to the comprehensive understanding of the synthesised uranyl nicotinate compound, including its synthesis yield, thermal behaviour, molecular composition, particle morphology, and elemental composition. The insights gained from this study can serve as a basis for further research in the field of inorganic chemistry, enabling the exploration of potential applications and the development of novel compounds with tailored properties.

Acknowledgments. This work is financially supported by the National Council for Scientific and Technological Development of Brazil (CNPq Process n°: 402435/2022-2) and by the

Financing Agency for Studies and Projects of Brazil (FINEP contract 04.13.0448.00/2013); the authors would like to thank the Group for Thermoanalytical Studies on Food, Drugs and Chemicals (dgp.cnpq.br/dgp/espelhogrupo/8922309087083951).

ИЗВОД

ИСПИТИВАЊЕ СВОЈСТАВА УРАНИЛ-НИКОТИНАТА: СИНТЕЗА, КАРАКТЕРИЗАЦИЈА И ТЕРМАЛНА АНАЛИЗА

MILEICKSON APARECIDO DE ASSIS PIRES, CLAUDIO TEODORO DE CARVALHO и TIAGO ANDRÉ DENCK COLMAN

Faculty of Exact Sciences and Technology – Federal University of Grande Dourados – UFGD, Dourados, Mato Grosso do Sul, Brazil

У овом раду описана је синтеза и карактеризација уранил-никотината, $UO_2(C_6H_4NO_2)_2{\cdot}0{,}25H_2O$. У синтези овог једињења метал и лиганд су реаговани у 1:2 молском односу у води као растварачу. Једињење је добијено у приносу од 67 %. Термогравиметријска анализа је показала да испитивано једињење постепено губи масу, што укључује дехидратацију, разлагање азота и редукцију UO_2^{2+}. На основу инфра-црвене спектроскопије потврђено је да је карбоксилна група у овом једињењу координована. Методом скенирајуће електронске микроскопије нађено је да су испитиване честице правилног овалног облика. Применом енергетски дисперзивне рендгенске спектроскопије нађено је да једињење садржи уранијум, угљеник, кисеоник и азот. Добијени резултати су од значаја за синтезу, термичка својства, састав, молекулску структуру и облик честица испитиваног једињења. Поред тога, приказани резултати могу бити од значаја за потенцијалну примену овог типа једињења.

(Примљено 17. августа, ревидирано 1. септембра, прихваћено 21. септембра 2023)

REFERENCES

1. G. Ş. Aşkın, H. Necefoğlu, G. Yılmaz Nayir, R. Çatak Çelik, T. Hökelek, *Acta Crystallogr., E* **71** (2015) 561 (https://doi.org/10.1107/S2056989015008270)
2. S. K. Verma, N. Bhojak, *Int. J. Chem. Phys. Sci.* **7** (2018) 67 (https://doi.org/10.30731/ijcps.7.2.2018.67-74)
3. M. Sertçelik, N. Delibas, H. Necefoğlu, T. Hökelek, *Acta Crystallogr., E* (2012) (https://doi.org/10.1107/s1600536812028814)
4. M. Sertçelik, B. Tercan, E. Şahin, H. Necefoğlu, T. Hökelek, *Acta Crystallogr., E* (2009) (https://doi.org/10.1107/s1600536809006047)
5. T. Hökelek, F. Yılmaz, B. Tercan, M. Sertçelik, H. Necefoğlu, *Acta Crystallogr., E* (2009) (https://doi.org/10.1107/s1600536809033200)
6. M. Sertçelik, N. Çaylak Delibaş, S. Çevik, H. Necefoğlu, T. Hökelek, *Acta Crystallogr., E* **68** (2012) m1196 (https://doi.org/10.1107/S1600536812035647)
7. G. Ş. Aşkın, H. Necefoğlu, S. Özkaya, R. Çatak Çelik, T. Hökelek, *Acta Crystallogr., E* **72** (2016) 888 (https://doi.org/10.1107/S2056989016008689)
8. G. Ş. Aşkın, H. Necefoğlu, A. M. Tonbul, N. Dilek, T. Hökelek, *Acta Crystallogr., E* **71** (2015) 479 (https://doi.org/10.1107/S2056989015006490)
9. V. A. Cocalia, M. P. Jensen, J. D. Holbrey, S. K. Spear, D. C. Stepinski, R. D. Rogers, *Dalton Transactions* (2005) 1966 (https://doi.org/10.1039/b502016f)

10. M. A. Degli-Esposti, P. J. Smolak, H. Walczak, J. Waugh, C.-P. Huang, R. F. DuBose, R. G. Goodwin, C. A. Smith, *J. Exp. Med.* **186** (1997) 1165 (https://doi.org/10.1084/jem.186.7.1165)
11. A. S. Ojo, S. Mamman, P. O. Ukoha, *J. Appl. Phys. Sci. Int.* (2022) 1 (https://doi.org/10.56557/japsi/2022/v14i17456)
12. D. Munz, *Organometallics* **37** (2018) 275 (https://doi.org/10.1021/acs.organomet.7b00720)
13. S.-S. Chen, *CrystEngComm* **18** (2016) 6543 (https://doi.org/10.1039/C6CE01258B)
14. H.-Z. Duan, C. Hu, Y.-L. Li, S.-H. Wang, Y. Xia, X. Liu, J. Wang, Y.-X. Chen, *J. Am. Chem. Soc.* **144** (2022) 22831 (https://doi.org/10.1021/jacs.2c09683)
15. K. Otake, H. Kitagawa, *Small* **17** (2021) 2006189 (https://doi.org/10.1002/smll.202006189)
16. P.-F. Yao, Y. Tao, H.-Y. Li, X.-H. Qin, D.-W. Shi, F.-P. Huang, Q. Yu, X.-X. Qin, H.-D. Bian, *Cryst. Growth Des.* **15** (2015) 4394 (https://doi.org/10.1021/acs.cgd.5b00724)
17. S. Dalai, M. Bera, A. Rana, D. S. Chowdhuri, E. Zangrando, *Inorg. Chim. Acta* **363** (2010) 3407 (https://doi.org/10.1016/j.ica.2010.06.043)
18. P. Thuéry, *Inorg. Chem. Commun.* **12** (2009) 800 (https://doi.org/10.1016/j.inoche.2009.06.021)
19. X. Kong, Y. Ren, L. Long, R. Huang, L. Zheng, *Inorg. Chem. Commun.* **10** (2007) 894 (https://doi.org/10.1016/j.inoche.2007.03.023)
20. G. T. Kent, J. Murillo, G. Wu, S. Fortier, T. W. Hayton, *Inorg. Chem.* **59** (2020) 8629 (https://doi.org/10.1021/acs.inorgchem.0c01224)
21. P. L. Arnold, D. Patel, C. Wilson, J. B. Love, *Nature* (2008) (https://doi.org/10.1038/nature06467)
22. A. Kumar, D. Lionetti, V. W. Day, J. D. Blakemore, *J. Am. Chem. Soc.* (2020) (https://doi.org/10.1021/jacs.9b11903)
23. J. A. Teixeira, W. D. G. Nunes, T. A. D. Colman, A. L. C. S. do Nascimento, F. J. Caires, F. X. Campos, D. A. Gálico, M. Ionashiro, *Thermochim. Acta* **624** (2016) 59 (https://doi.org/10.1016/j.tca.2015.11.023)
24. F. O. Farias, A. C. Jasko, T. A. D. Colman, L. A. Pinheiro, E. Schnitzler, A. C. Barana, I. M. Demiate, *Braz. Arch. Biol. Technol.* **57** (2014) 821 (https://doi.org/10.1590/S1516-8913201402506)
25. F. X. Campos, A. L. C. S. Nascimento, T. A. D. Colman, D. A. Gálico, A. C. S. Carvalho, F. J. Caires, A. B. Siqueira, M. Ionashiro, *Thermochim. Acta* **651** (2017) 73 (https://doi.org/10.1016/j.tca.2017.03.002)
26. T. A. D. Colman, D. J. C. Gomes, F. J. Caires, O. T. Filho, R. de C. da Silva, M. Ionashiro, *J. Anal. Appl. Pyrolysis* **111** (2015) 132 (https://doi.org/10.1016/j.jaap.2014.11.021)
27. A. L. C. S. do Nascimento, F. J. Caires, T. A. D. Colman, D. J. C. Gomes, G. Bannach, M. Ionashiro, *Thermochim. Acta* **604** (2015) 7 (https://doi.org/10.1016/j.tca.2014.12.022)
28. T. A. D. Colman, D. J. C. Gomes, F. J. Caires, O. T. Filho, R. de C. da Silva, M. Ionashiro, *Thermochim. Acta* **591** (2014) 111 (https://doi.org/10.1016/j.tca.2014.06.013)
29. A. S. de Souza, B. Ekawa, C. T. de Carvalho, J. A. Teixeira, M. Ionashiro, T. A. D. Colman, *Thermochim. Acta* **683** (2020) 178443 (https://doi.org/10.1016/j.tca.2019.178443)

30. K. V. Tenório, J. A. Teixeira, L. M. de Campos Pinto, F. J. Caires, O. Treu-Filho, F. A. dos Santos, T. A. Denck Colman, A. Cuin, C. T. de Carvalho, *J. Rare Earths* **36** (2018) 1090 (https://doi.org/10.1016/j.jre.2018.03.019)
31. M. D. Colman, S. R. da S. Lazzarotto, M. Lazzarotto, F. A. Hansel, T. A. D. Colman, E. Schnitzler, *J. Anal. Appl. Pyrolysis* **119** (2016) 157 (https://doi.org/10.1016/j.jaap.2016.03.005)
32. J. A. Teixeira, W. D. G. Nunes, A. L. C. S. do Nascimento, T. A. D. Colman, F. J. Caires, D. A. Gálico, M. Ionashiro, *J. Anal. Appl. Pyrolysis* **121** (2016) 267 (https://doi.org/10.1016/j.jaap.2016.08.0060)
33. C. D. Bet, C. S. de Oliveira, T. A. D. Colman, R. Z. B. Bisinella, C. Beninca, L. G. Lacerda, A. P. Ramos, E. Schnitzler, *J. Therm. Anal. Calorim.* **138** (2019) 2733 (https://doi.org/10.1007/s10973-019-08374-7)
34. C. D. Bet, C. S. de Oliveira, T. A. D. Colman, M. T. Marinho, L. G. Lacerda, A. P. Ramos, E. Schnitzler, *Food Chem.* **264** (2018) 435 (https://doi.org/10.1016/j.foodchem.2018.05.021)
35. C. A. Schneider, W. S. Rasband, K. W. Eliceiri, *Nat. Methods* **9** (2012) 671 (https://doi.org/10.1038/nmeth.2089)
36. Y. Yang, J. Liu, Y. Sun, S. Hu, Y. Gao, Z. Zhang, S. Luo, L. Rao, *J. Chem. Thermodyn.* **113** (2017) 350 (https://doi.org/10.1016/j.jct.2017.07.002)
37. J. A. Teixeira, W. D. G. Nunes, A. L. C. S. do Nascimento, T. A. D. Colman, F. J. Caires, D. A. Gálico, M. Ionashiro, *J. Anal. Appl. Pyrolysis* **121** (2016) 267 (https://doi.org/10.1016/j.jaap.2016.08.006)
38. G. Deacon, *Coord. Chem. Rev.* **33** (1980) 227 (https://doi.org/10.1016/S0010-8545(00)80455-5)
39. F. X. Campos, A. L. C. S. Nascimento, T. A. D. Colman, D. A. Gálico, O. Treu-Filho, F. J. Caires, A. B. Siqueira, M. Ionashiro, *J. Therm. Anal. Calorim.* **123** (2016) 91 (https://doi.org/10.1007/s10973-015-4956-7)
40. M. A. Abu-Dalo, N. A. F. Al-Rawashdeh, I. R. Al-Mheidat, N. S. Nassory, *IOP Conf. Ser. Mater. Sci. Eng.* **92** (2015) 012023 (https://doi.org/10.1088/1757-899X/92/1/012023).